ADVANCED BIOSYSTEMS
www.adv-biosys.com

The Prismatic Topography of *Pinctada maxima* Shell Retains Stem Cell Multipotency and Plasticity In Vitro

*Enateri V. Alakpa, Anwer Saeed, Peter Chung, Mathis O. Riehle, Nikolaj Gadegaard, Matthew J. Dalby, and Maggie Cusack**

The shell of the bivalve mollusc *Pinctada maxima* is composed of the calcium carbonate polymorphs calcite and aragonite (nacre). Mother-of-pearl, or nacre, induces vertebrate cells to undergo osteogenesis and has good osteointegrative qualities in vivo. The calcite counterpart, however, is less researched in terms of the response of vertebrate cells. This study shows that isolation of calcite surface topography from the inherent chemistry allows viable long-term culture of bone marrow derived mesenchymal stem cells (MSCs). Self-renewal is evident from the increased gene expression of the self-renewal markers CD63, CD166, and CD271 indicating that cells cultured on the calcite topography maintain their stem cell phenotype. MSCs also retain their multipotency and can undergo successful differentiation into osteoblasts and adipocytes. When directed to adipogenesis, MSCs cultured on prism replicas are more amenable to differentiation than MSCs cultured on tissue culture polystyrene indicating a higher degree of plasticity in MSCs growing on calcite *P. maxima* prismatic topography. The study highlights the potential of the calcite topography of *P. maxima* as a biomimetic design for supporting expansion of MSC populations in vitro, which is of fundamental importance if it meets the demands for autologous MSCs for therapeutic use.

1. Introduction

Chemical, mechanical, and topographical features are well known characteristics which provide active cues within the cellular niche, guiding behavioral processes such as functionality,[1] cell migration,[2] differentiation,[3] and maintaining the self-renewal property of stem cells.[3b,4] as such, these characteristics play an important role in the design and development of biocompatible materials able to direct and sustain any number of cellular functions for tissue engineering applications.

Biomineralization is the process by which organisms sequester simple inorganic components to create hardened tissue types. In nature, these structures accomplish a range of functions including photoreception,[5] gravity sensing and balance,[6] defense against predation in invertebrate shells, and support in vertebrate skeletons. In vertebrates, calcium phosphate is used to form bones and teeth. Invertebrate systems such as corals and shells utilize calcium carbonate which can be assembled in a number of ways generating a staggering amount of structural diversity.[7] A small (5%) component of the shell is organic matrix which drives and orchestrates the biomineralization process.[8] These are responsible for the assembly and mineralization of each of the calcium carbonate polymorphs such as calcite and aragonite, resulting in their very distinct overall composite structures.[9] This "phosphate-carbonate break" in genealogical similarity

Dr. E. V. Alakpa
Institution for Integrative Medical Biology
Umeå University
SE901 87 Umeå, Sweden
Dr. A. Saeed, Prof. N. Gadegaard
Division of Biomedical Engineering
School of Engineering
University of Glasgow
Glasgow G12 8LT Scotland, UK

The ORCID identification number(s) for the author(s) of this article can be found under https://doi.org/10.1002/adbi.201800012.

DOI: 10.1002/adbi.201800012

P. Chung
School of Geographical & Earth Sciences
College of Science & Engineering
Gregory Building
University of Glasgow
Glasgow G12 8QQ, UK
Dr. M. O. Riehle, Prof. M. J. Dalby
Centre for Cell Engineering
Institute of Molecular Cell & Systems Biology
College of Medical
Veterinary & Life Sciences
Joseph Black Building
University of Glasgow
Glasgow G12 8QQ, UK
Prof. M. Cusack
Division of Biological & Environmental Sciences
Faculty of Natural Sciences
Cottrell Building
University of Stirling
Stirling FK9 4LA, UK
E-mail: maggie.cusack@stir.ac.uk

and compatibility of vertebrate and invertebrate biominerals, known as the bone-shell divide is curiously bridged by mother of pearl or nacre. Nacre possesses good osteoinductive[10] and integrative qualities[11] with its topography alone able to induce bone formation in mesenchymal stem cells (MSCs).[10a]

By contrast, the calcite layer of many bivalve shells has been little studied in terms of the inherent characteristics of the calcite prisms, and the effect that these highly defined surface features may have on eliciting reactions in mammalian cells. The biocompatibility of human bone marrow derived MSCs with invertebrate biominerals (shells)[10b,12] raises the question of whether the response of mammalian cells to some shell biominerals is due to the inherent chemistry, topography or a combination of both and to what extent either characteristic able to influence cell behavior.

As previously stated, the chemical, mechanical, and topographical characteristics of the cellular microenvironment are crucial to influencing cell behavior both in vivo and in vitro. Additionally, studies have also shown that these characteristics are also capable of acting independently of one another to direct cell fate in vitro. Outside of their natural environment, signaling cues are lost and stem cells lose their ability to self-renew and differentiate.[13] Therefore, biomaterials that are able to sustain the stem cell phenotype are highly desirable.[14]

For this reason, calcite and its inherent properties still leaves a number of facets to explore in relation to tissue engineering applications.

We have previously reported that nacre topography, independent of its chemistry, is able to elicit osteogenesis in MSCs.[10a] Here we isolate the calcite prism topography from its innate chemistry, hypothesizing that calcite topography is able to support stem cell survival and thus influence subsequent cell behavior. To this end, we demonstrate that calcite topography has much to offer in stem cell and tissue engineering research.

2. Results

2.1. Fidelity of Replica Prism Topography

Scanning electron microscopy (SEM) digital elevation models of replicate nanopatterns of the calcite surfaces onto polycaprolactone (PCL) polymer confirmed the high fidelity of the prism replicas (**Figure 1**b,c). Mean surface roughness measurements of the replicate prismatic surface showed good agreement when compared to the original shell prisms and values were not significantly different with good pattern replication from the shell (462 ± 46 nm) to the PCL counterpart (407.8 ± 14 nm), giving a measured fidelity better than 84% (Figure 1b). The prismatic envelopes (white arrow in Figure 1c), being deeper channels are less well replicated than the prism surface and their loss of definition contributes to the overall smoothing effect of the replication.

2.2. MSC Gene Expression on Replica Prism Topography

Gene transcription levels of mesenchyme tissue biomarkers, e.g., CD63 (self-renewal), PPAR-γ (adipogenesis), MyoD (myogenesis), SOX-9 (chondrogenesis), and OPN (osteogenesis) were initially determined at two weeks using quantitative real-time PCR and again after five weeks in culture on planar (control) and prismatic PCL replica substrates. MSCs cultured on the prismatic replicas showed little activity at two weeks with a small increased average for CD63 expression (×1.61). After five weeks in culture, differences in gene expression on each substrate were more pronounced. Cells cultured on the prismatic topography had a statistically significant increase in CD63 expression, suggestive of stem cell phenotype retention after five weeks (**Figure 2**a). There were no statistically significant changes in PPAR-γ (adipocyte), MyoD (myoblast), osteopontin (osteoblast), and SOX-9 (chondrocyte) expression indicating lack of lineage specification.

Gene expression responses of MSCs to prismatic replicas were compared to MSCs response to nacre replicas where, consistent with previous studies, and unlike the prismatic surfaces, nacre replicas supported increased gene expression for the bone marker osteopontin (OPN).

To confirm the increase in gene expression indicative of self-renewal (CD63) on prism replicas and bone production (OPN) on nacre replicas, gene expression levels of additional self-renewal (CD166 and CD271) and osteogenic (OSX and ONN) markers were also measured. These followed the trend observed in the initial screen confirming retention of stem cell phenotype on the prismatic topography and promotion of osteogenesis on nacre topography (Figure 2b,c).

To confirm lack of functional differentiation on the prismatic surface, cell cultures were assessed immunofluorescently for myogenin, fatty acid binding protein (FABP4), and OPN, indicative of myogenesis, adipogenesis, and osteogenesis, respectively. Cells did not show any indication of mature development along any lineage but retained STRO-1 expression, again confirming retention of a multipotent phenotype (**Figure 3**). Positive controls using defined myogenic, adipogenic, and osteogenic media showed the MSCs potential to differentiate. Further, it is noteworthy that MSCs on control, planar surfaces did not express either self-renewal or differentiation markers. This indicates fibroblastic overgrowth on the planar control surfaces, which is a major issue for in vitro MSC culture.[3b]

2.3. Preservation of MSC Phenotype Is Topography Driven

Initial assessment of phenotype preservation was based on three cell surface markers: CD63, CD166, and CD271. This set of self-renewal markers provides indications of phenotypic shifts which are then analyzed in more detail in terms of differentiation potential. Short-term (72 h) cell seeding experiments show that MSCs seeded directly onto calcite prisms would preferentially localize to the prismatic envelope rather than the calcite prism itself (**Figure 4**a,b). However, when seeded onto the PCL replica, cells are evenly dispersed across the substrate without any location bias (Figure 3). This indicates that prism topography does not impede cell proliferation but that the inherent chemistry of the calcite prisms impedes cell attachment and growth.

To ascertain whether the surface chemistry takes precedence over topography in influencing expression of self-renewal markers (CD63, CD166, and CD271), cells were presented with

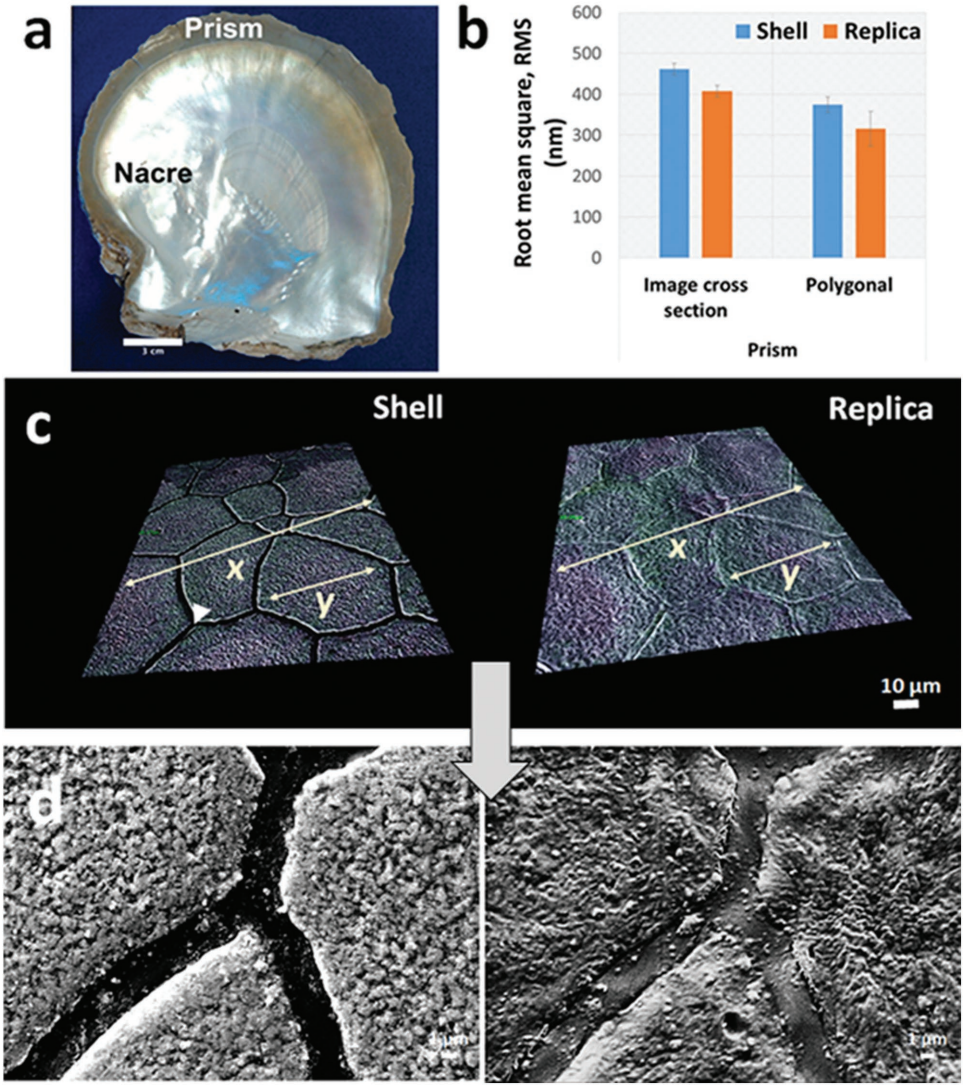

Figure 1. Fidelity of replica prismatic topography. a) Internal view of a single valve of a *Pinctada maxima* shell showing the nacreous and prismatic surface regions. b) Average surface roughness (RMS) of the prismatic region of the shell and c) its polymer replica measured using digital elevation models from scanning electron microscopy images of the shell prismatic regions and their equivalent replicated PCL regions. d) Corresponding high magnification images. Measurements to determine average surface roughness ($n = 6$) were taken at random cross-sections across the entire image (x) as well as within single polygons on the prism (y). The arrows indicate the location of the interprismatic envelope. Error bars in B denote standard deviation from the mean; scale bar in a) 3 cm, c) 10 µm, and d) 1 µm.

the shell calcite (Pr) and prism polymer replicas (PrR) as well as these two substrates coated with gold (Au-Pr and Au-PrR) or titanium (Ti-Pr and Ti-PrR). This approach presents the cells with altered surface chemistries that are biocompatible but are predicted to invoke different cell reactions. Shell and PCL substrates were coated with gold (Au-Pr and Au-PrR), which is biocompatible and elicits cell behavior akin to glass substrates which are often used as a control substrate having no discernible effect on general cell culture behavior.[15] Surfaces were coated with titanium (Ti-Pr and Ti-PrR), which induces cell adhesion.[15a,16]

MSCs cultured on the uncoated PrR substrate again showed increased expression of all three self-renewal biomarkers (CD63, CD166, and CD271) compared to the planar PCL control supporting the results obtained in Figure 2a,b. By contrast, cells cultured on the Pr substrate showed the opposite effect with CD63 and CD166 expression downregulated and CD271 nondiscernible from the control confirming that, while the shell itself does not support phenotypic maintenance, the topography does.

MSCs cultured on the gold coated substrates (shell and replicas), showed an increase in all three self-renewal markers compared to the control (Figure 4c). Expression levels for cells cultured on uncoated (PrR) and gold-coated (Au-PrR) prism replicas for all three markers were comparable indicating that there was no significant difference in cell response on the uncoated or gold-coated prism replicas. The gold-coated shell calcite (Au-Pr) also showed increased expression of the

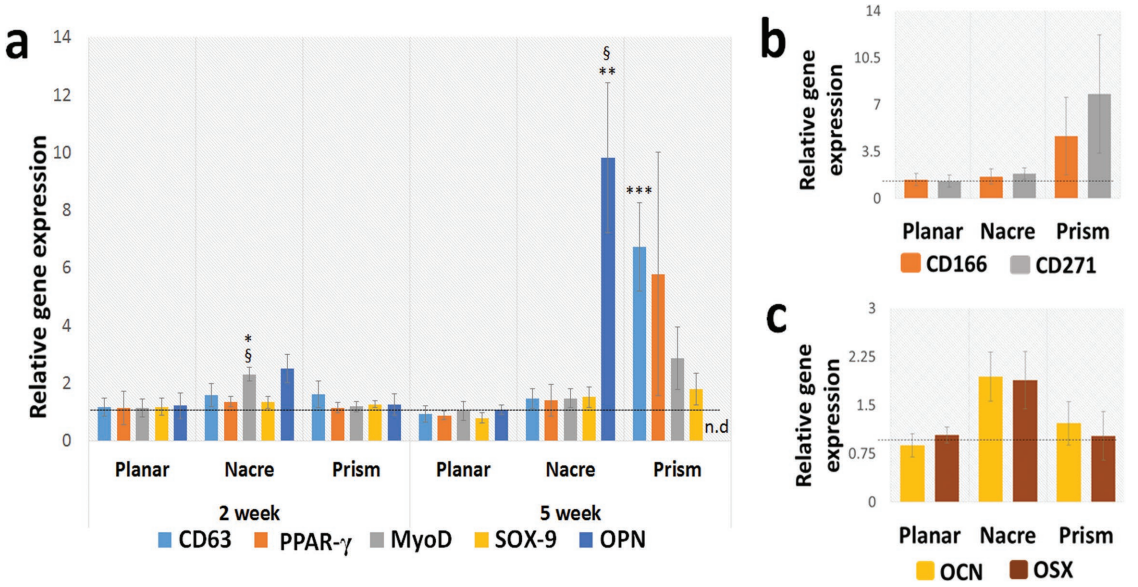

Figure 2. Gene transcription expression of MSCs cultured on the prismatic replicates. a) Cells were first assessed for indication of self-renewal (CD63) as well as differentiation (PPAR-γ, MyoD, SOX-9, and OPN) into typical mesenchyme tissue types. After five weeks, the prismatic topography showed significant increase in CD63 and no detectable levels of OPN, this is in contrast to the typically osteogenic nacre. b) Analysis of expression of additional self-renewal markers ALCAM and CD271 by MSCs cultured on the shell replicate topographies after five weeks in culture. MSCs showed increased expression on the prismatic pattern while the nacre remained unchanged from the control. c) When assessed for osteogenic markers (OSX and OCN) after five weeks, the nacre pattern retains osteoinductive properties showing an increase in expression of osteogenic markers while the prismatic remains unchanged from the control confirming that prism topography is not osteoinductive and supports MSC self-renewal in vitro. Dashed line represents the control (planar) which is held nominally at 1. Error bars denote standard errors from the mean. * indicates statistical significance compared to the planar substrate and § indicates statistical significance comparing prism and nacre substrates where $p < 0.05$ as calculated using one way ANOVA and Tukey's post hoc tests; $n = 6$.

self-renewal markers and is in stark contrast to the observed effect of the uncoated shell material (Pr). Expression levels of CD63 and CD166 were comparable to levels observed for the replica substrates PrR and Au-PrR. CD271 levels, although higher than the planar control, was significantly less than expression levels on the replica substrates (Figure 4c).

Cells cultured on the titanium-coated surfaces did not show increased expression of CD63, CD166, or CD271 (Figure 4c). Average levels of expression for all three self-renewal markers were 0.49× the planar control for the shell coated substrate (Ti-Pr), showing a negative trend comparable with the uncoated calcite (0.58×). Average levels for the Ti-coated replica substrate (Ti-PrR) however were closer to the control (0.83×, the control is held nominally at 1.0 for all three markers).

2.4. Directed Differentiation of MSCs Cultured on the Prismatic Topography

Although MSCs are defined by the expression of a number of surface markers including STRO-1, ALCAM, CD63/HOP26, and melanoma cell adhesion molecule (CD146), these alone are not sufficient to determine multipotency. The fundamental attribute of cellular multipotency should also be demonstrated through directed differentiation into fat, muscle, cartilage or bone tissue.[17] Here we show that MSCs maintained in culture on the replica prismatic topography are able to undergo directed differentiation into both adipogenic and osteogenic tissue types. MSCs seeded onto the prismatic replicas were maintained in culture for four weeks. Following this, cells were detached and replated into normal tissue culture well plates. Cells were then differentiated along adipogenic and osteogenic lineages using defined induction media[17b,18] for 28 d. Adipocyte differentiation was successfully induced as indicated by positive oil red staining of lipid droplets and immunofluorescent staining of fatty acid binding protein (FABP4) (**Figure 5**a–e). Osteogenic differentiation of MSCs was also successfully achieved as evidenced from increased alizarin red staining and immunofluorescent staining for osteocalcin (Figure 5f–k).

Semiquantitative comparisons of differentiation efficiency between MSCs maintained on prismatic substrates and on culture well plastic indicate that MSCs cultured on the prismatic substrates were more adept at forming adipose cells than were cells maintained on culture well plastic (Figure 5e). Osteogenic development was the same for cells maintained on prism replicas as cells maintained on culture well plastic substrates (Figure 5k).

3. Discussion and Conclusions

That MSCs are highly responsive to the topography features of their microenvironment is well documented. We have demonstrated that, while calcite prisms of *Pinctada maxima* shells are bioincompatible, the topography of the calcite prisms is biocompatible. Prism topography may provide a starting point from which to identify surface characteristics that promote the maintenance of multipotency. In this study we have

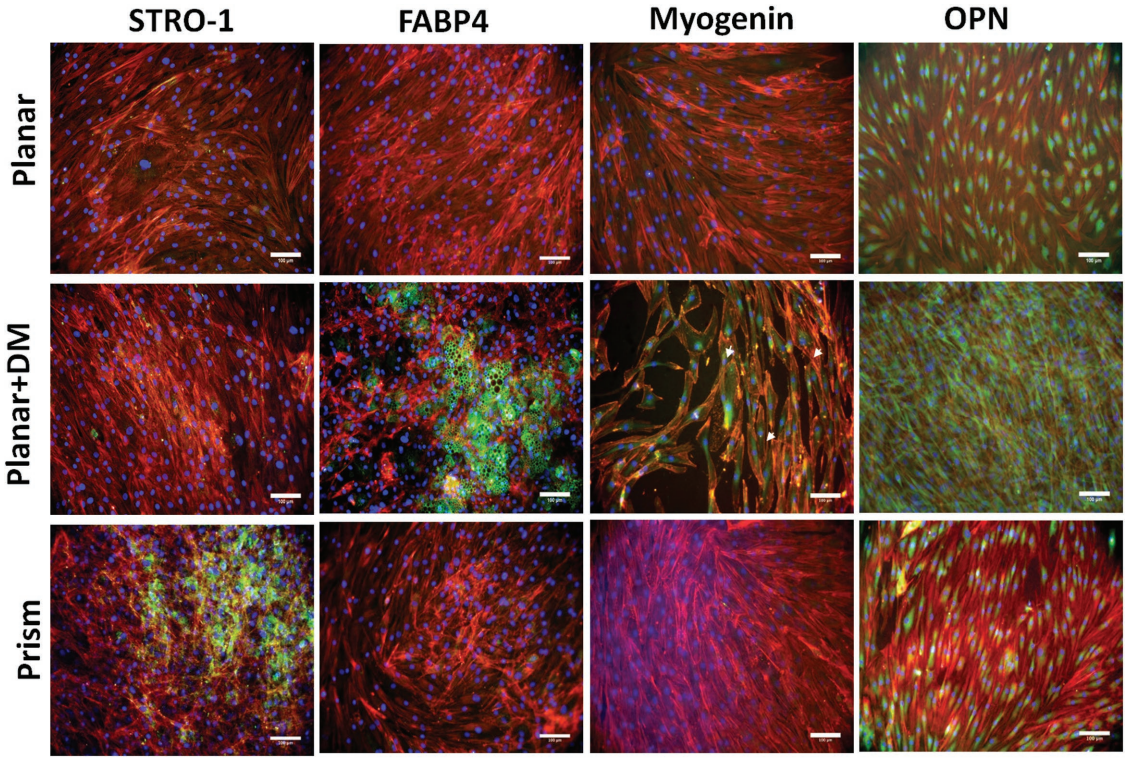

Figure 3. Immunofluorescence microscopy of MSCs cultured on PCL prismatic substrates. Fluorescence staining was carried out to affirm the gene expression data as well as confirm lack of differentiation into other mesenchyme lineages. MSCs were cultured on planar PCL surfaces in the absence or presence of lineage specific differentiating media (+DM) as negative and positive controls, respectively, as well as the prismatic replicas. Cells in lot STRO-1/Planar+DM were maintained in basal media for the experiment duration, as there is no defined media for stem cell retention. Cells on the prismatic topography stained positively for STRO-1 only, confirming multipotency retention. Although an increase in transcription was measured there is no indication of further differentiation in adipose (fatty acid binding protein (FABP4)), muscle (myogenin) or bone (OPN) cell types. Cells were stained for cell nucleus (blue), f-actin (red), and each named lineage biomarker (green). Scale bars: 100 µm.

shown that isolation of prismatic topography from its inherent chemistry triggers a different response in MSCs compared to its osteoinductive nacre counterpart. Growth on the prism replicas facilitates self-renewal and maintains plasticity. Unlike the shell prisms, prism replicas do not impede cell attachment and growth. This impediment is due to the inherent chemistry of the prisms as supported by the use of alternative chemistries thin-coated onto the prismatic topographies. Gold and titanium are both biocompatible and they affect cell behavior in different ways. Comparisons between MSCs cultured on the Au-Pr and Au-PrR substrates indicate that the degree of loss in replication fidelity of the prismatic topography from the shell to PCL (Figure 1) does not have any significant effect on expression levels of CD63 and CD166 but that CD271 expression may be more sensitive to the loss of surface roughness. It highlights the idea that some surface markers are expressed at different levels due to subtle differences in their microenvironment accounting for the general heterogeneity that is often observed with stem cell characterization as a whole.[17a,19] Titanium is a biomaterial widely used in dental surgery and orthopaedic applications due to its ability to support osteogenic development of stem cells as it is highly cell adherent.[20] That MSCs lost markers of multipotency is thus sensible as preservation of MSC multipotency in culture has been linked to lowering adhesion.[21] Therefore, so long as the surface topography remains the primary signaling cue, and chemistry does not override, then the MSC phenotype can be retained.[22] The results also highlight the fact that, although the topography supports phenotype retention, the chemistry can also be important in eliciting this response.

In addition to increased biocompatibility on the prism replicas instead of calcite prisms, MSCs also conserved their stem cell phenotype and multipotency characteristics when maintained on prismatic replica substrates. When directed to differentiate into adipose tissue, MSCs maintained on prism replicas were more amenable than cells kept on cell culture plastic indicating greater plasticity of MSCs maintained on prism topography than on cell culture plastic.

Out of their niche, on cell culture plastic, MSCs lack the information that they require to grow and maintain multipotency and so tend to differentiate, mainly into fibroblasts.[3b] This differentiation reduces the ability to provide MSC scale up for autologous therapies and tissue engineering applications. Cells that were cultured on the planar and prismatic substrates were both able to undergo directed adipogenesis and osteogenesis. A crucial difference between the two, however, is that the cells that had spent time on the prismatic substrate were more amenable to adipogenesis than those from the planar culture well plastic. This response to directed differentiation after being maintained on a hard substrate is indicative of retained

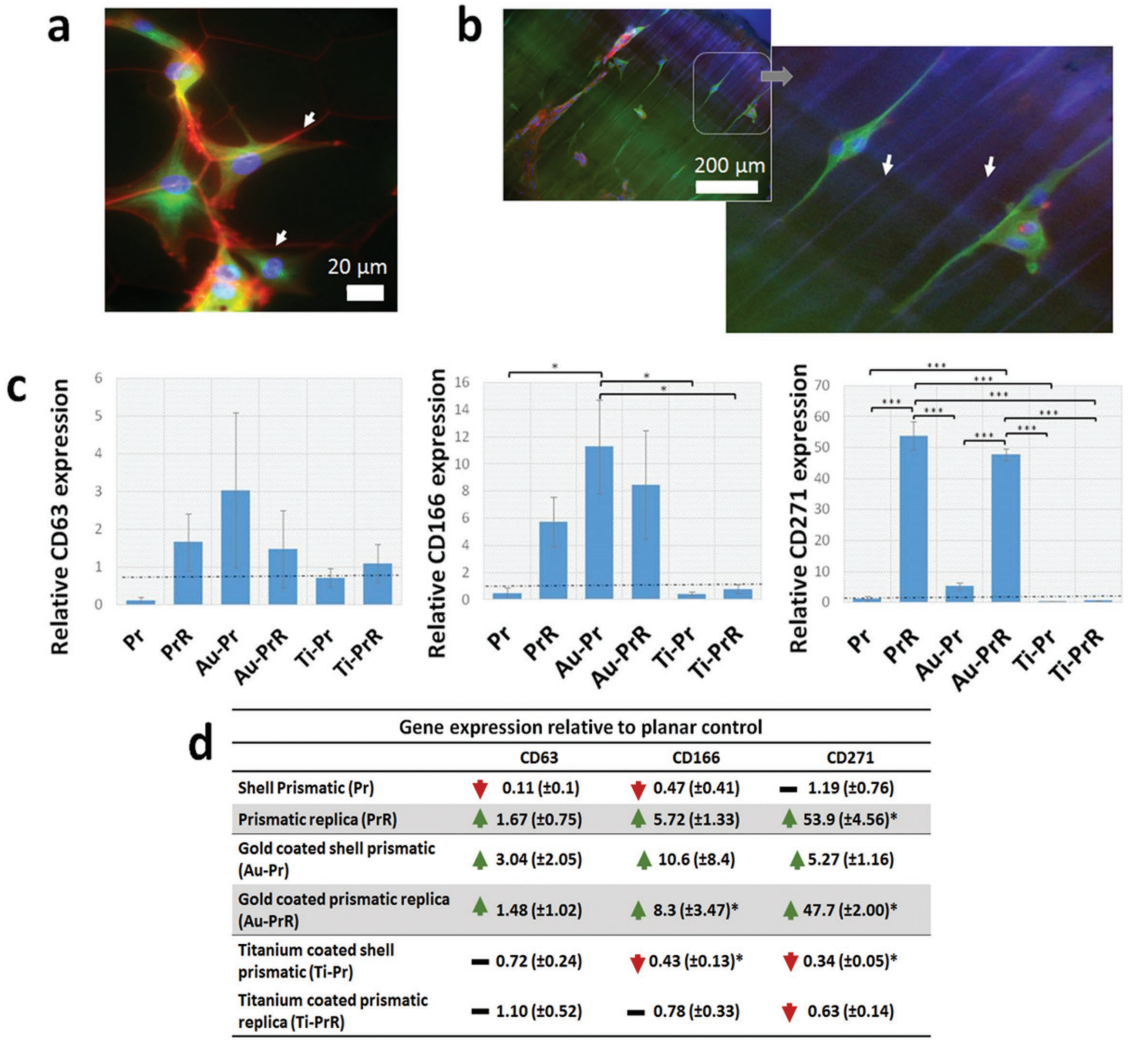

d

Gene expression relative to planar control	CD63	CD166	CD271
Shell Prismatic (Pr)	▼ 0.11 (±0.1)	▼ 0.47 (±0.41)	▬ 1.19 (±0.76)
Prismatic replica (PrR)	▲ 1.67 (±0.75)	▲ 5.72 (±1.33)	▲ 53.9 (±4.56)*
Gold coated shell prismatic (Au-Pr)	▲ 3.04 (±2.05)	▲ 10.6 (±8.4)	▲ 5.27 (±1.16)
Gold coated prismatic replica (Au-PrR)	▲ 1.48 (±1.02)	▲ 8.3 (±3.47)*	▲ 47.7 (±2.00)*
Titanium coated shell prismatic (Ti-Pr)	▬ 0.72 (±0.24)	▼ 0.43 (±0.13)*	▼ 0.34 (±0.05)*
Titanium coated prismatic replica (Ti-PrR)	▬ 1.10 (±0.52)	▬ 0.78 (±0.33)	▼ 0.63 (±0.14)

Figure 4. Comparison of MSC behavior on shell and replica prismatic surfaces. Fluorescently stained cells cultured on the prismatic shell for 72 h show that calcite prisms do not support cell adhesion and the cells adhere mainly to the interprismatic envelope (a – top surface and b – lateral surface). Interprismatic envelope is shown with the arrows). c) Gene expression profiles of MSC multipotency markers cultured for three weeks on prismatic calcite (Pr), prismatic topography replicated onto PCL (PrR) and both calcite prisms and replicas coated with either gold (Au-Pr and Au-PrR) or titanium (Ti-Pr and Ti-PrR). Cells cultured on Pr showed negative expression of all three self-renewal markers relative to the control. PrR in contrast show increased levels of all three markers as do cells cultured on both gold-coated surfaces. MSCs cultured on the titanium-coated surfaces do not show increased expression levels indicating a loss of phenotype on this surface. Error bars denote standard errors from the mean; Dashed line indicates the planar PCL control which is held nominally at 1; * indicates statistical significance where $p < 0.05$ as calculated using one way ANOVA followed by Tukey's post hoc test; $n = 4$. Cells in (a) and (b) were stained for cell nucleus (blue), f-actin (red), and β-tubulin (green). Scale bar in (a) 20 µm and (b) 200 µm.

multipotency, as hard substrates will be more amenable to osteogenesis than adipogenesis.[23]

Stem cells isolated from bone marrow are characteristically heterogeneous, with different proliferative characteristics and therefore the exact mechanisms regulating self-renewal are still poorly understood. Mechanotransductive effects from the cell-material interphase via focal adhesion complexes are directly linked to the cell nucleus and thus have a direct effect on stem cell lineage commitment.[24] Surface feature characteristics that are able to restrict the formation of large or mature focal adhesion complexes cause a low tensile state within the cell. A number of pathways are considered to be activated in response to mechanotransductive effects inclusive of Ras/MAPK, RhoA/ROCK, PI3k/Akt, and TGF-β facilitating cell differentiation or renewal.[25] Also noteworthy, is that low tensile states likewise cause MSCs to undergo adipogenesis,[26] and where the fault line between adipogenesis and self-renewal lies is not known. It is considered likely that one or more of these pathways are involved with phenotype retention of cells and as several topographies supporting self-renewal are discovered, they can contribute to our understanding of the mechanisms.

While osteogenesis is quite well understood in terms of topographical, mechanical, and chemical requirements from the work with hydroxyapatite and bioglass in the 1980s through to the surface engineering paradigms of the last decade,[3a,26b,27] MSC growth and self-renewal is much less well understood and few examples of surfaces that promote growth without differentiation exist.[3b,28] As such, the calcite prismatic component of

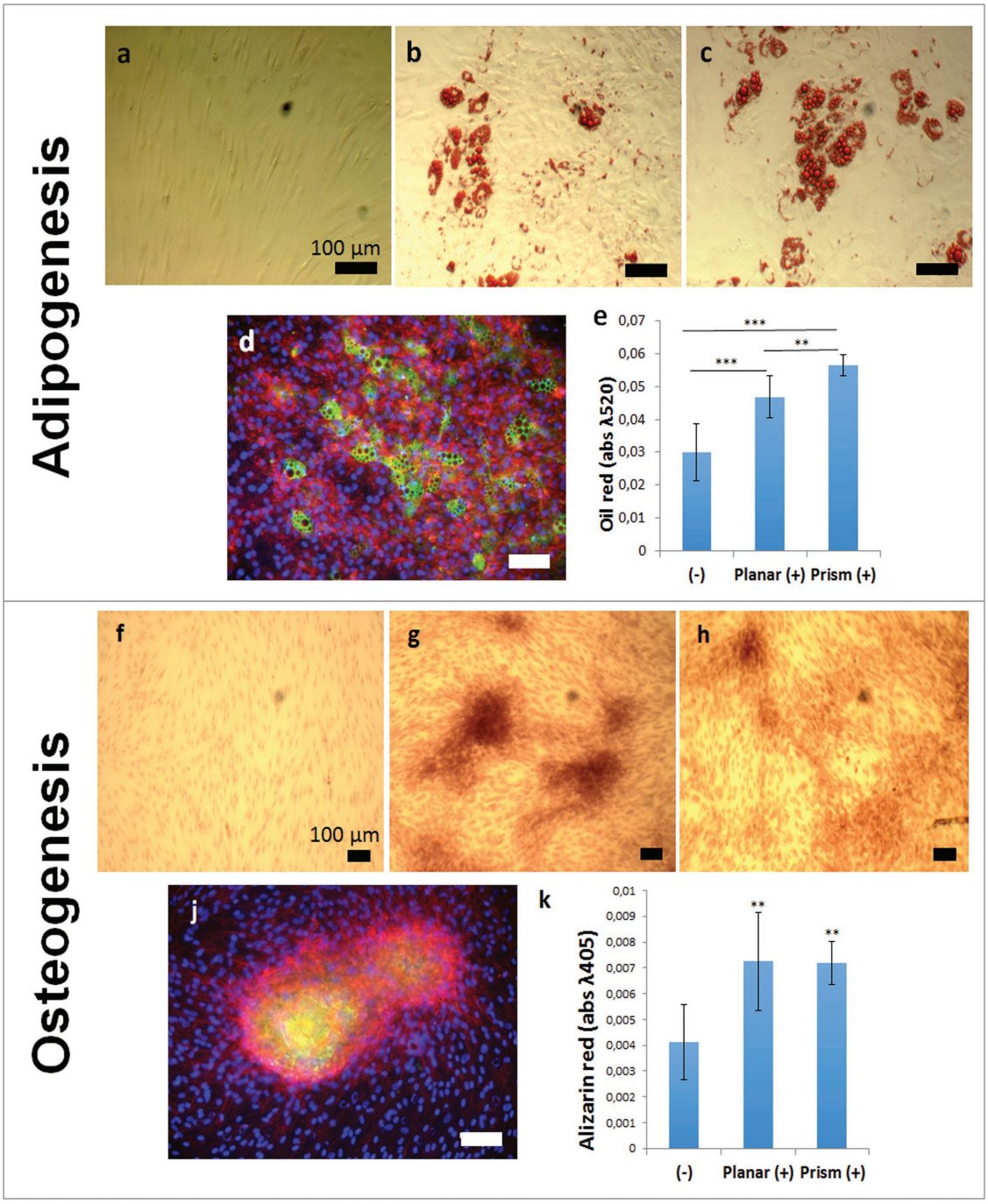

Figure 5. Directed differentiation of MSCs after maintenance on prismatic replica substrates. MSCs were differentiated into either adipose or osteoblast cells and stained using oil red and alizarin red respectively to demonstrate the multipotency of cells acquired from the prismatic replica substrate. Cells were cultured in a,f) the absence of differentiation media as controls. b,g) MSCs collected from culture well plastic and c,d,h,j) the prismatic topographies were cultured in differentiation media. e,k) Total dye content from histologically stained samples was determined using UV spectroscopy and compared to undifferentiated cell populations (–). Cells sourced and differentiated from the prismatic substrate were also fluorescently stained for FABP4 (d) and osteocalcin (j), indicating adipogenesis and osteogenesis, respectively. Scale bars: 100 µm. Error bars in (e) and (k) denote standard deviations from the mean; * indicates statistical significance where $p < 0.05$ as calculated using one way ANOVA and Tukey's post hoc tests; $n \geq 4$.

the pearl oyster shell is a promising potential source of bioinspiration for the development of biomaterial design to maintain the growth properties of stem cells and provide autologous stem cells for therapeutic applications.

4. Experimental Section

Fabrication of Shell Replica Substrates: Shells were rinsed and sonicated in distilled water for 10 min and then washed in 70% ethanol prior to use for replica fabrication and cell seeding.

Inverse or negative patterns were fabricated onto polydimethylsiloxane (PDMS stamps) by curing a 1:10 PDMS (Sylgard 184, Dow Corning) mixture (degassed prior to use) at 60 °C for 1 h. Replicas were subsequently made using PCL beads, which had been washed in methanol and air dried. These were melted at 80 °C on a hot plate and the hard baked PDMS stamps then pressed into the PCL. Samples were then removed and cooled to ≈21 °C (room temperature) thus allowing the PCL to solidify. Finally, the stamp was peeled away from the PCL, leaving behind the positive shell surface replica.

Scanning Electron Microscopy and Digital Elevation Modeling: Shells were cut to ≈1 × 1 cm^2 and their PCL replicas were coated with a thin layer of carbon and mounted to SEM stubs prior to imaging. Two images were taken at 0° and 5° stage tilt of each substrate and 3D images created using digital elevation modeling. The surface roughness was calculated as the deviation from the averaged base line of the shell or its replica respectively. SEM imaging and digital elevation modeling were carried out on a Quanta 200 (FEI) scanning electron microscope and Alicona Mex 5.1 software in the Imaging, Spectroscopy and Analysis Centre (ISAAC) at the School of Geographical and Earth Sciences at the University of Glasgow.

Gold and Titanium Coating of Shell and Replica Surfaces: Shells cut to ≈1 × 1 cm^2 and their PCL replicas (also a sq. cm) were coated with gold (Au) or titanium (Ti) using physical vapor deposition. An E-beam evaporator was used to coat 5 nm titanium and 10 nm of gold, respectively (n = 4 replicates) with 0.3 nm s^{-1} deposition rate in the low 10^{-7} mbar vacuum chamber (Playss IV). Coating thicknesses were kept to a maximum of 10 nm, which is the general range used for SEM imaging and ensures that the topography is kept intact.

Cell Culture: Human mesenchymal stem cells obtained from purified bone marrow (Promocell, GmBH) were cultured and maintained at 37 °C and 5% CO_2 atmosphere in DMEM culture media supplemented with 100×10^{-6} M sodium pyruvate, 0.8×10^{-3} M L-glutamine, 10% foetal bovine serum (FBS), and 1% of penicillin–streptomycin (10 mg mL^{-1} solution) of the total volume. This supplemented DMEM culture mix was used for all cell culture procedures unless stated otherwise.

Cells were subcultured when ≈80–90% confluent by incubating with trypsin for ≈5 min to detach the adherent cells from the culture flask. The action of trypsin was then halted by the addition of an equal volume of culture media and the resulting cell suspension transferred into 20 mL flasks and centrifuged for 5 min at 1400 g to sediment the cells. The trypsin/media supernatant was then decanted to waste and the cells resuspended in an appropriate volume of fresh media (cell numbers used in subsequent experiments were maintained at $\approx 1.5 \times 10^4$ cells unless otherwise stated). Cells were then either seeded into another culture flask and allowed to grow confluent as the subsequent passage or used for pending experiments. Cells used for all ensuing experiments were between passage 1 and 3 and media changes were performed twice weekly. PCL replica substrates were subject to plasma cleaning (Harrick Plasma) for 1.5 min, washed in 70% ethanol and rinsed with culture media prior to cell seeding.

Directed differentiation of MSCs was accomplished by supplementing standard DMEM culture media with tailored cocktails of inducing agents. These were used as positive controls to compare with test substrates. Cells were seeded at high confluence (80–90%) prior to differentiation. Adipogenic differentiation was induced using induction media constituting 1 µm dexamethasone, 1.7 µm insulin, 200 µm indomethacin, and 500 µm isobutylmethylxanthine[18,29] in DMEM. This was alternated with DMEM containing 1.7 µm insulin[18a,29b] as a maintenance media at regular intervals. Osteogenic differentiation was induced using DMEM containing 10% FBS, dexamethasone (100×10^{-9} M), and ascorbate-2-phosphate (350×10^{-6} M). Cells were then maintained at 37 °C in differentiation media and the media changed twice weekly for the duration of the experiment. Myogenic differentiation was induced using 0.1×10^{-6} M dexamethasone, and 50×10^{-6} M hydrocortisone in DMEM.[18b]

Quantitative PCR Analysis: RNA extractions of cells cultured in plastic well plates were done using the RNeasy microkit (Qiagen) as per manufacturer's protocol. Reverse transcription was carried out using the QuantiTect reverse transcription kit (Qiagen) as per the manufacturer's instructions. Resultant cDNA samples were then stored at −20 °C or used immediately for qRT-PCR experiments.

Human specific primers designed to detect a number of differentiation biomarkers was done using the universal probe library assay design centre available from Roche Applied Sciences.[30] PCR was carried out using a 7500 real-time PCR system and corresponding software (Applied Biosystems, UK). Samples had a total reaction volume of 20 µL containing 2 µL of cDNA, each reverse and forward primer at a final concentration of 100×10^{-6} M and analyzed using SYBR green chemistry. Samples were held at 50 °C for 2 min then 95 °C for 10 min then amplified using 95 °C for 15 s and 60 °C for 1 min for 40 cycles. The specificity of the PCR amplification was checked with a heat dissociation curve (measured between 60 and 95 °C) subsequent to the final PCR cycle. Gene expression levels were standardized using glyceraldehyde-3-phosphate dehydrogenase (GAPDH) as an internal control. Quantification analysis was performed using the comparative $\Delta\Delta Ct$ method[31] and gene expression calculated as fold change relative to the defined control sample. Details of the PCR primers used within this chapter are given in **Table 1**.

Histology and Fluorescence Staining: Alizarin red staining of osteogenic cultures was done using an 8.3×10^{-3} M solution of alizarin red dissolved in distilled water. The pH was adjusted to 4.2 with 5 M sodium hydroxide and passed through a 0.2 µm filter. Culture media was aspirated to waste and the cells washed once with 500 µL of phosphate buffered saline (PBS). After washing, 500 µL of 10% formalin in PBS (fixative) was added to each well and incubated at ≈21 °C for 20 min after which the cells were then washed twice for 5 min on a shaker with distilled water. Following this, 500 µL of alizarin red solution was added to each culture well and incubated at 21 °C for 30 min. Cells were then washed with distilled water repeatedly until the liquid was clear. Samples were stored in PBS solution at 4 °C until ready for viewing under a microscope.

Table 1. Real-time PCR primers used to quantify mRNA expression from human genes.

Gene		
ALCAM	Forward	5′-ACG ATG AGG CAG CAG AGA TAA GT-3′
	Reverse	5′-CAG CAA GGA GGA GAC CAA CAA C-3′
CD63	Forward	5′-GCT GTG GGG CTG CTA ACT AC-3′
	Reverse	5′-ATC CCA CAG CCC ACA GTA AC-3′
CD271	Forward	5′-TCA TCC CTG TCT ATT GCT CCA-3′
	Reverse	5′-TGT TCT GCT TGC AGC TGT TC-3′
PPAR-γ	Forward	5″-TGT GAA GCC CAT TGA AGA CA-3″
	Reverse	5′-CTG CAG TAG CTG CAC GTG TT-3′
MyoD	Forward	5′-CAC TAC AGC GGC GAC TCC-3′
	Reverse	5′-TAG GCG CCT TCG TAG CAG-3′
SOX-9	Forward	5′-AGA CAG CCC CCT ATC GAC TT-3′
	Reverse	5′-CGG CAG GTA CTG GTC AAA CT-3′
OPN	Forward	5′-AGC TGG ATG ACC AGA GTG CT- 3′
	Reverse	5′-TGA AAT TCA TGG CTG TGG AA -3′
OCN	Forward	5′-CAG CGA GGT AGT GAA GAG ACC-3′
	Reverse	5′-TCT GGA GTT TAT TTG GGA GCA G-3′
OSX	Forward	5′-GCT TAT CCA GCC CCC TTT AC -3′
	Reverse	5′-CAC TGG GCA GAC AGT CAG AA -3′
GAPDH	Forward	5′-ACC CAG AAG ACT GTG GAT GG-3′
	Reverse	5′-TTC TAG ACG GCA GGT CAG GT-3′

Oil red staining of adipogenic cultures was done using a 4.4×10^{-3} M working solution, consisting of three parts oil red (7.34×10^{-3} M stock in propan-2-ol) to two parts distilled water and passed through a 0.2 µm filter. Culture media was aspirated to waste and the cells washed once with 500 µL of PBS. Cells were then fixed with 10% formalin in PBS for 20 min at 21 °C. Following this, 500 µL of 60% propanol was added to each well and incubated at 21 °C for ≈3 min. The propanol solution was then aspirated to waste and an equal volume of oil red working solution added to the culture wells and incubated at 21 °C for 5 min. Cells were then washed with distilled water repeatedly until the liquid was clear.

Cultures on glass cover slips and PCL substrates used for fluorescence imaging were rinsed once in PBS and fixed at 37 °C with 10% formalin in PBS for 15 min. They were then permeabilized with 0.5% Triton X in PBS and blocked using 1% BSA in PBS. Following this, cells were incubated at 37 °C for an hour with rhodamine-conjugated phalloidin and the required primary antibody). After 1 h, cells were washed three times for 5 min with 0.5% tween 20 in PBS and incubated for an hour at 37 °C with the corresponding secondary antibody. Cells were again washed thrice with 0.5% Tween in PBS, incubated at 4 °C for 30 min with streptavidin conjugated FITC and washed again as before after the incubation time elapsed. Samples were then mounted onto a drop of Vectashield-DAPI (a glycerol based mounting medium for preserving fluorescence containing DAPI for nucleic acid staining) on a microscope slide. For biomaterial substrates, Vectashield-DAPI was diluted in PBS and added to the well plates. All samples were stored at 4 °C wrapped in foil to protect from photobleaching until ready for viewing under a microscope.

UV/Vis Spectroscopy: MSCs differentiated along the adipogenic lineage, which had been stained with oil red, were destained for ≈5 min monitored under a light microscope with methanol. After this, the methanol was removed from the well plate, transferred to clean Eppendorf tubes and the solution absorbance quantified at wavelength 520 nm using a nanodrop ND-1000 spectrophotometer and software (Nanodrop technologies Inc. Wilmington, USA).

Extraction of alizarin red for spectrometry was done as described by Gregory et al.[32] Cells were detached by incubating with 200 µL 10% acetic acid for 30 min on a shaker. The solution was then transferred into clean Eppendorf tubes, vortexed and heated for 10 min at 85 °C. Samples were then cooled on ice for 5 min and centrifuged for 15 min at 13 000 rpm to sediment any debris. Following this, the pH of the supernatant adjusted to 4.2 using 10% ammonium hydroxide solution. The absorbance was then quantified at wavelength 405 nm using a nanodrop spectrometer. Undifferentiated (negative control) cells were also stained with either oil red or alizarin red were and taken through the described process for comparison

Statistical Analysis: Unpaired Student's *t*-tests were carried out using Microsoft Excel for comparisons between two test groups. Analysis of variance (ANOVA) followed by Tukey's post hoc tests were performed using GraphPad Prism software (version 6.03) to compare more than two study groups. Statistical significance is noted where the calculated probability that the null hypothesis is true (*p*-value) is less than 5% confident (0.05).

Raw data generated from this study is available from the University of Glasgow library depository at http://dx.doi.org/10.5525/gla.researchdata.346.

Acknowledgements

This work was funded by the Medical Research Council (MRC) grant MR/K011278/1 "Stem cell metabolomics for bone therapies and tissue engineering." The authors thank Bernie Degnan and Carmel McDougall of the University of Queensland, and Patrick Moase of Clipper Pearls Pty Ltd for provision of *Pinctada maxima* shells.

Conflict of Interest

The authors declare no conflict of interest.

Keywords

biominerals, calcite, self-renewal, stem cells, topography

Received: January 9, 2018
Revised: February 15, 2018
Published online: April 24, 2018

[1] a) Y. S. Choi, L. G. Vincent, A. R. Lee, M. K. Dobke, A. J. Engler, *Biomaterials* **2012**, 33; b) B. WojciakStothard, A. Curtis, W. Monaghan, K. Macdonald, C. Wilkinson, *Exp. Cell Res.* **1996**, *223*, 426.

[2] E. Korpos, C. Wu, J. Song, R. Hallmann, L. Sorokin, *Cell Tissue Res.* **2010**, *339*, 47.

[3] a) M. J. Dalby, N. Gadegaard, R. Tare, A. Andar, M. O. Riehle, P. Herzyk, C. D. W. Wilkinson, R. O. C. Oreffo, *Nat. Mater.* **2007**, *6*, 997; b) R. J. McMurray, N. Gadegaard, P. M. Tsimbouri, K. V. Burgess, L. E. McNamara, R. Tare, K. Murawski, E. Kingham, R. O. C. Oreffo, M. J. Dalby, *Nat. Mater.* **2011**, *10*, 637; c) W. Y. Tong, W. Shen, C. W. F. Yeung, Y. Zhao, S. H. Cheng, P. K. Chu, D. Chan, G. C. F. Chan, K. M. C. Cheung, K. W. K. Yeung, Y. W. Lam, *Biomaterials* **2012**, *33*, 7686.

[4] a) F. Chowdhury, Y. Z. Li, Y. C. Poh, T. Yokohama-Tamaki, N. Wang, T. S. Tanaka, *Plos One* **2010**, *5*, e15655; b) S. Gerecht, J. A. Burdick, L. S. Ferreira, S. A. Townsend, R. Langer, G. Vunjak-Novakovic, *Proc. Natl. Acad. Sci. USA* **2007**, *104*, 11298.

[5] J. Aizenberg, A. Tkachenko, S. Weiner, L. Addadi, G. Hendler, *Nature* **2001**, *412*, 819.

[6] R. W. Gauldie, *J. Morphol.* **1993**, *218*, 1.

[7] M. Cusack, A. Freer, *Chem. Rev.* **2008**, *108*, 4433.

[8] a) M. J. Almeida, C. Milet, J. Peduzzi, L. Pereira, J. Haigle, M. Barthelemy, E. Lopez, *J. Exp. Zool.* **2000**, *288*, 327; b) M. Kono, N. Hayashi, T. Samata, *Biochem. Biophys. Res. Commun.* **2000**, *269*, 213.

[9] B. Marie, C. Joubert, A. Tayale, I. Zanella-Cleon, C. Belliard, D. Piquemal, N. Cochennec-Laureau, F. Marin, Y. Gueguen, C. Montagnani, *Proc. Natl. Acad. Sci. USA* **2012**, *109*, 20986.

[10] a) E. V. Alakpa, K. E. V. Burgess, P. Chung, M. O. Riehle, N. Gadegaard, M. J. Dalby, M. Cusack, *ACS Nano* **2017**, *11*, 6717; b) D. W. Green, H.-J. Kwon, H.-S. Jung, *Mol. Cells* **2015**, *38*, 267.

[11] a) G. Atlan, N. Balmain, S. Berland, B. Vidal, E. Lopez, *C. R. Acad. Sci., Ser. III* **1997**, *320*, 253; b) E. Lopez, G. Atlan, S. Berland, N. Balmain, *Bone (New York)* **1997**, *20*, 107S.

[12] A. Flausse, C. Henrionnet, M. Dossot, D. Dumas, S. Hupont, A. Pinzano, D. Mainard, L. Galois, J. Magdalou, E. Lopez, P. Gillet, M. Rousseau, *J. Biomed. Mater. Res. A* **2013**, *101*, 3211.

[13] F. Ulloa-Montoya, C. M. Verfaillie, W. S. Hu, *J. Biosci. Bioeng.* **2005**, *100*, 12.

[14] S. M. Dellatore, A. S. Garcia, W. M. Miller, *Curr. Opin. Biotechnol.* **2008**, *19*, 534.

[15] a) L. Raisanen, M. Kononen, J. Juhanoja, P. Verpavaara, J. Hautaniemi, J. Kivilahti, M. Hormia, *J. Biomed. Mater. Res.* **2000**, *49*, 9; b) E. P. Ivanova, J. Hasan, H. K. Webb, V. K. Truong, G. S. Watson, J. A. Watson, V. A. Baulin, S. Pogodin, J. Y. Wang, M. J. Tobin, C. Löbbe, R. J. Crawford, *Small* **2012**, *8*, 2489.

[16] E. Lautenschlager, P. Monaghan, *Int. Dent. J.* **1993**, *43*, 9.

[17] a) M. Dominici, K. Le Blanc, I. Mueller, I. Slaper-Cortenbach, F. C. Marini, D. S. Krause, R. J. Deans, A. Keating, D. J. Prockop, E. M. Horwitz, *Cytotherapy* **2006**, *8*, 315; b) M. F. Pittenger, A. M. Mackay, S. C. Beck, R. K. Jaiswal, R. Douglas, J. D. Mosca, M. A. Moorman, D. W. Simonetti, S. Craig, D. R. Marshak, *Science* **1999**, *284*, 143.

[18] a) L. Janderova, M. McNeil, A. N. Murrell, R. L. Mynatt, S. R. Smith, *Obes. Res.* **2003**, *11*, 65; b) P. A. Zuk, M. Zhu, H. Mizuno, J. Huang, J. W. Futrell, A. J. Katz, P. Benhaim, H. P. Lorenz, M. H. Hedrick, *Tissue Eng.* **2001**, *7*, 211.
[19] R. S. Tare, J. C. Babister, J. Kanczler, R. O. C. Oreffo, *Mol. Cell. Endicrinol.* **2008**, *288*, 11.
[20] a) E. Dawson, G. Mapili, K. Erickson, S. Taqvi, K. Roy, *Advanced Drug Delivery Reviews* **2008**, *60*, 215; b) S. Oh, K. S. Brammer, Y. S. J. Li, D. Teng, A. J. Engler, S. Chien, S. Jin, *Proc. Natl. Acad. Sci. USA* **2009**, *106*, 2130.
[21] P. Tsimbouri, N. Gadegaard, K. Burgess, K. White, P. Reynolds, P. Herzyk, R. Oreffo, M. J. Dalby, *J. Cell. Biochem.* **2014**, *115*, 380.
[22] S. Britland, C. Perridge, M. Denyer, H. Morgan, A. Curtis, C. Wilkinson, *Exp. Biol. Online* **1997**, *1*, 1.
[23] C. Yang, M. W. Tibbitt, L. Basta, K. S. Anseth, *Nat. Mater.* **2014**, *13*, 645.
[24] a) M. M. Nava, M. T. Raimondi, R. Pietrabissa, *J. Biomed. Biotechnol.* **2012**, https://doi.org/10.1155/2012/797410; b) P. M. Tsimbouri, K. Murawski, G. Hamilton, P. Herzyk, R. O. C. Oreffo, N. Gadegaard, M. J. Dalby, *Biomaterials* **2013**, *34*, 2177.
[25] M. J. Dalby, N. Gadegaard, R. O. C. Oreffo, *Nat. Mater.* **2014**, *13*, 558.
[26] a) F. Guilak, D. M. Cohen, B. T. Estes, J. M. Gimble, W. Liedtke, C. S. Chen, *Cell Stem Cell* **2009**, *5*, 17; b) R. McBeath, D. M. Pirone, C. M. Nelson, K. Bhadriraju, C. S. Chen, *Dev. Cell* **2004**, *6*, 483.
[27] D. S. W. Benoit, M. P. Schwartz, A. R. Durney, K. S. Anseth, *Nat. Mater.* **2008**, *7*, 816.
[28] a) J. M. Curran, R. Stokes, E. Irvine, D. Graham, N. A. Amro, R. G. Sanedrin, H. Jamil, J. A. Hunt, *Lab Chip* **2010**, *10*, 1662; b) P. M. Gilbert, K. L. Havenstrite, K. E. G. Magnusson, A. Sacco, N. A. Leonardi, P. Kraft, N. K. Nguyen, S. Thrun, M. P. Lutolf, H. M. Blau, *Science* **2010**, *329*, 1078.
[29] a) S. Mirmalek-Sani, R. Tare, S. M. Morgan, H. Roach, D. Wilson, N. Hanley, R. C. Oreffo, *Stem Cells* **2006**, *24*, 12; b) D. J. Klemm, J. W. Leitner, P. Watson, A. Nesterova, J. E. B. Reusch, M. L. Goalstone, B. Draznin, *J. Biol. Chem.* **2001**, *276*, 28430.
[30] RocheAppliedSciences, https://qpcr.probefinder.com/roche3.html (accessed: March 2013).
[31] J. H. Schefe, K. E. Lehmann, I. R. Buschmann, T. Unger, H. Funke-Kaiser, *J. Mol. Med.* **2006**, *84*, 901.
[32] C. A. Gregory, W. G. Gunn, A. Peister, D. J. Prockop, *Anal. Biochem.* **2004**, *329*, 77.